Research Square

Preprints are preliminary reports that have not undergone peer review.
They should not be considered conclusive, used to inform clinical practice,
or referenced by the media as validated information.

Prognostic Analysis of Iodine-avid Residual Metastatic Lymph Nodes in Differentiated Thyroid Cancer

Ruoxin Xu
The Fifth Affiliated Hospital, Sun Yat-Sen University
Qingyuan Jia
The Fifth Affiliated Hospital, Sun Yat-Sen University
Mingxuan Zhao
The Fifth Affiliated Hospital, Sun Yat-Sen University
Qiyong Pan
The Fifth Affiliated Hospital, Sun Yat-Sen University
Caihua Tang
tangcaih@mail.sysu.edu.cn

The Fifth Affiliated Hospital, Sun Yat-Sen University https://orcid.org/0009-0000-5851-5945

Research Article

Keywords: Differentiated thyroid cancer, Radioiodine therapy, Lymph node metastasis, Treatment response, Nomogram

Posted Date: October 14th, 2026

DOI: https://doi.org/10.21203/rs.3.rs-11024915/v1

License: This work is licensed under a Creative Commons Attribution 4.0 International License.
Read Full License

Abstract

Backgroud

: In clinical practice, even with equivalent administered radioiodine(^{131}I) activities, metastatic lymph node lesions exhibit heterogeneous responses to initial ^{131}I therapy among differentiated thyroid cancer (DTC)patients.

Objectives

To evaluate the efficacy of initial ^{131}I treatment in DTC patients with iodine-avid residual metastatic lymph nodes (reLNs) and to develop a model for predicting the functional ^{131}I therapy response.

Methods

220 DTC patients who underwent initial ^{131}I therapy with iodine-avid reLNs on Rx-WBS (post-therapy whole-body scan with SPECT/CT) were included retrospectively in this study. Imaging features of reLNs, including number, maximum short-axis diameter, calcification, and semiquantitative ^{131}I uptake indices, together with pre-therapy stimulated thyroglobulin (ps-Tg) and administrated ^{131}I activity were analyzed. ^{131}I therapy response was assessed according to the 2015 American Thyroid Association criteria. Functional ^{131}I therapy response was defined as two groups by disappearance or persistence of iodine uptake on reLNs according to the follow-up scans. To predict the functional ^{131}I therapy response, logistic regression was used to identify independent predictors and a nomogram was constructed and validated.

Results

After initial ^{131}I therapy, patients exhibited excellent response (ER, 44.5%), indeterminate response (IDR, 30.0%), biochemically incomplete response (IR, 11.4%), and structurally incomplete response (SIR,14.1%), respectively. In terms of functional outcomes, 86.8% of patients had complete resolution of radioactive iodine uptake, while persistent iodine uptake was observed in the remaining 13.2% of cases. Compared with the disappearance group, the persistent ^{131}I uptake group had higher administrated ^{131}I activity, higher ps-Tg levels, more iodine-avid lymph nodes, larger maximum short-axis diameter and more frequent calcification of the reLNs. Multivariable analysis identified ps-Tg and number of iodine-avid reLNs as independent risk factors for ^{131}I persistent uptake. In the imaging-only model, lymph node number and maximum short-axis diameter were positively associated with ^{131}I persistent uptake. The nomogram achieved an AUC of 0.792 (95% CI, 0.678–0.906).

Conclusion

Initial ^{131}I therapy yielded favorable outcomes in DTC patients with iodine-avid reLNs. The number and size of reLNs serve as key predictors of persistent radioactive iodine uptake. A novel nomogram incorporating ps-Tg, metastatic nodal number, and maximum short-axis diameter was constructed to preliminarily achieve individualized prediction of functional therapeutic response.

1. Introduction

Differentiated thyroid cancer (DTC) generally has a favorable prognosis, but cervical lymph node metastasis and postoperative residual disease remain important causes of persistent disease and structural recurrence. Radioiodine (^{131}I) therapy is widely used after surgery for remnant ablation, adjuvant therapy, or treatment of known disease. In recent years, domestic and international guidelines have increasingly emphasized individualized decision-making regarding the indication and administered activity of ^{131}I therapy rather than routine treatment for all patients (1, 2). However, even among patients with the same TNM stage or recurrence risk category, response to ^{131}I therapy and long-term outcomes may vary substantially, suggesting that clinicopathological risk stratification alone is insufficient for precise individualized management (3).

The burden, distribution, and aggressive features of metastatic lymph nodes are closely associated with recurrence risk in DTC. Previous studies have shown that a larger number of metastatic lymph nodes, greater nodal size, wider nodal distribution, and more aggressive pathological features are associated with a higher risk of local structural recurrence and shorter recurrence-free survival (4–6). Post-therapy whole-body scan with SPECT/CT (Rx-WBS) after ^{131}I therapy can identify iodine-avid residual metastatic lymph nodes (reLNs) and provide both functional and anatomical information. Nevertheless, most previous studies have mainly focused on whether lymph node lesions are iodine-avid, whereas quantitative or semiquantitative uptake characteristics and morphological features, such as nodal number, short-axis diameter, calcification, and distribution, have rarely been integrated to predict treatment response.

In clinical practice, even with equivalent administered ^{131}I activities, metastatic lymph node lesions exhibit heterogeneous responses to initial radioiodine therapy among DTC patients: some patients achieve complete resolution of iodine uptake, while others present with persistent uptake or novel emergence of iodine-avid lesions. This heterogeneity may reflect differences in tumor burden and radioiodine sensitivity, but the imaging and clinical factors associated with persistent iodine uptake after ^{131}I therapy remain unclear. Therefore, this retrospective study included postoperative DTC patients with definite iodine-avid reLNs on Rx-WBS after initial ^{131}I therapy. We evaluated the associations of reLN number, maximum short-axis diameter, calcification, nodal distribution, relative iodine avidity, and clinical indicators such as pre-therapy stimulated thyroglobulin (ps-Tg) with treatment response, especially functional ^{131}I therapy response defined by persistence or disappearance of nodal iodine uptake. A

nomogram model was further developed to predict persistent iodine uptake after ^{131}I therapy, aiming to provide a quantitative tool for individualized treatment optimization and follow-up stratification.

2. Materials and Methods

2.1 Patient selection

This retrospective study was approved by the Ethics Committee of The Fifth Affiliated Hospital of Sun Yat-sen University(Approval No. (2025) K141-1).

Patients with postoperative DTC who underwent initial ^{131}I therapy in the Department of Nuclear Medicine, The Fifth Affiliated Hospital of Sun Yat-sen University, between September 1, 2020 and January 31, 2024 were enrolled in this study. Inclusion criteria were: total or near-total thyroidectomy with lymph node dissection, pathologically confirmed DTC, intermediate- or high-risk disease according to the ATA recurrence risk stratification system (7), iodine-avid cervical or mediastinal reLNs on post-therapy whole-body scan with SPECT/CT (Rx-WBS), and at least 12 months of follow-up. Patients with other malignancies, incomplete clinical or imaging data, or additional treatment between surgery and ^{131}I therapy were excluded.

Clinical and pathological variables, including age, sex, pathological type, tumor size, extrathyroidal extension, nodal status, distant metastasis, AJCC 8th TNM stage(8), ATA risk stratification, pre-therapy stimulated thyroglobulin (ps-Tg), TgAb, and administered ^{131}I activity, were collected. Serum TSH, Tg, and TgAb were measured using Roche assays, with measurable ranges of 0.005-100 μIU/mL, 0.04–5000 ng/mL, and 0-4000 IU/mL, respectively.

2.2 ^{131}I therapy and imaging protocol

Before ^{131}I therapy, all patients underwent thyroid hormone withdrawal and a low-iodine diet for 2–4 weeks until endogenous TSH reached ≥ 30 mIU/L. ^{131}I activity was individually determined according to postoperative risk stratification, pathological stage, tumor burden, laboratory findings, and imaging results, with reference to the 2015 ATA guidelines and Chinese guidelines (9). The administered activity ranged from 1.11 to 7.40 GBq (30–200 mCi). Rx-WBS with SPECT/CT was performed 2–5 days after ^{131}I administration. During follow-up, diagnostic whole-body scintigraphy (Dx-WBS) and/or the second post-therapy scan were performed to assess the persistence of radioiodine avidity in previously iodine-avid lymph nodes. Additional imaging, including neck ultrasonography, CT/MRI, chest CT, bone scintigraphy, or ^{18}F-FDG PET/CT, was performed when clinically indicated.

2.3 Therapy Response Evaluation of ^{131}I therapy

Therapeutic efficacy following initial ^{131}I therapy was assessed via two complementary approaches. First, overall ^{131}I therapy response was assessed according to the 2015 ATA response-to-therapy system and classified as excellent response (ER), indeterminate response (IDR), biochemical incomplete

response (BIR), or structural incomplete response (SIR) (7). This classification was used to describe the general clinical response of each patient by integrating biochemical and imaging findings.

Second, a functional ^{131}I therapy response assessment was performed based on the iodine uptake status of metastatic lymph nodes during follow-up. The primary functional outcome was whether persistent iodine uptake existed in metastatic lymph nodes after ^{131}I therapy. Patients were stratified into two groups based on follow-up diagnostic whole-body scintigraphy (Dx-WBS) and/or second post-therapy whole-body scintigraphy (Rx-WBS): the iodine uptake disappearance group and the persistent iodine uptake group. For patients undergoing a single session of ^{131}I therapy, the initial Rx-WBS findings were compared with Dx-WBS results. For those receiving two cycles of ^{131}I therapy, the initial and second Rx-WBS findings were compared. In cases of discrepant results between Dx-WBS and the second Rx-WBS, grouping classification was determined by the findings of the second Rx-WBS. (10).

2.4 Imaging Analysis of reLNs on Rx-WBS

Iodine-avid reLNs were defined as abnormal extra-thyroid-bed iodine uptake on Rx-WBS corresponding to nodal-like structures on SPECT/CT. For each patient,the number of reLNs, maximum short-axis diameter on axial CT, presence of calcification, involved region, and semiquantitative iodine uptake indices were recorded. Regional involvement was categorized as single-region involvement, multi-region involvement, or mediastinal involvement (11, 12).

For semiquantitative analysis, the maximum voxel value of each reLN was measured on fused SPECT/CT images. A spherical VOI of approximately 1 cm³ was placed in the mediastinal blood pool at the level of the ascending aorta on the pulmonary artery bifurcation slice, avoiding vessel walls, adjacent high-uptake structures, and artifacts (13). Another VOI with the same shape and size as the lesion VOI was placed in contralateral normal soft tissue on the same slice. The lymph node-to-mediastinal blood pool ratio and lymph node-to-contralateral soft-tissue ratio were calculated. Because the ratios were right-skewed, log10 transformation was applied before statistical analysis (14).

2.5 Model construction and statistical analysis

Patients were divided into the iodine uptake disappearance group and persistent iodine uptake group according to the functional outcome. Continuous variables were expressed as mean±standard deviation or median with interquartile range, and categorical variables as numbers and percentages. Between-group comparisons were performed using the Mann-Whitney U test for continuous variables, and Fisher’s exact test for categorical variables, as appropriate.

Serum Tg values below the limit of detection (0.04 ng/mL) were entered as LOD/2, whereas values above the upper limit of quantification (5000 ng/mL) were entered as the upper limit. Variables with $P \le 0.10$ in univariable analysis and clinically relevant variables were entered into multivariable logistic regression to identify independent predictors of persistent iodine uptake. A nomogram was constructed based on selected predictors (15). Statistical analyses were performed using SPSS version 27.0 and R software with the rms package. A two-sided $P < 0.05$ was considered statistically significant. To evaluate the

discrimination and calibration of the nomogram model, internal validation was performed using bootstrap resampling. With 500 bootstrap repetitions, calibration curves were plotted to compare the predicted probabilities with observed outcomes, and Harrell's C statistic (C-index) and the area under the receiver operating characteristic curve (AUC) were calculated to assess discrimination. Decision curve analysis (DCA) was performed to compare the net benefit of the model across different threshold probabilities. Finally, clinical decision curves were generated in R to evaluate the clinical utility of the model.

3. Results

3.1 Clinical Characteristics of the Patients

A total of 220 patients were included. The median age at DTC diagnosis was 42 years, and 146 patients (66.4%) were female. Most patients had papillary thyroid carcinoma (218/220, 99.1%), and 2 patients (0.9%) had follicular thyroid carcinoma. The median administered activity for initial ^{131}I therapy was 120 mCi, and the median pre-therapy ps-Tg level was 9.1 ng/mL. Detailed baseline characteristics are summarized in Table 1.

Table 1
Clinical characteristics of the patients

Clinical characteristics	Median/Mean (range/standard deviation) / number (ratio)
Gender	
Female	146 (66.4%)
Male	74 (33.6%)
Age at diagnosis (years)	42 (18 ~ 74)
Histology	
PTC	218 (99.1%)
FTC	2 (0.9%)
Tumor size (mm)	15.0 (2 ~ 70)
Tumor laterality	
Ipsilateral	148 (67.3%)
Bilateral	72 (32.7%)
Cervical lymph node surgery	
Central	91 (41.3%)
Central+ Lateral	129 (58.7%)
T status	
T1	125 (56.8%)
T2	32 (14.5%)
T3	45 (20.5%)
T4	15 (6.8%)
Tx	3 (1.4%)
N status	
N0	10 (4.5%)
N1	210 (95.5%)
Distant metastasis	1(0.5%)
AJCC TNM	

Note: ATA, American Thyroid Association; AJCC, American Joint Committee on Cancer; ps-Tg, pre-therapy stimulated thyroglobulin; PTC, papillary thyroid carcinoma; FTC, Follicular carcinomoa.

Clinical characteristics	Median/Mean (range/standard deviation) / number (ratio)
	187(85.0%)
	27(12.3%)
	6(2.7%)
I-131 activity (mCi)	120(30 ~ 200)
ATA risk stratification	
Intermediate risk	184(83.6%)
High risk	36(16.4%)
Pre-therapy ps-Tg (ng/mL)	9.1(0.02 ~ 5000)
Note: ATA, American Thyroid Association; AJCC, American Joint Committee on Cancer; ps-Tg, pre-therapy stimulated thyroglobulin; PTC, papillary thyroid carcinoma; FTC, Follicular carcinomoa.	

Table 1

3.2 ^{131}I Therapy Response Evaluation

After initial ^{131}I therapy, 98 patients (44.5%) attained ER, 66 patients (30.0%) achieved IDR, 25 patients (11.4%) exhibited BIR, and 31 patients (14.1%) showed SIR. Overall, 74.5% of patients achieved an acceptable response (ER + IDR) (Fig. 1A). In terms of functional iodine uptake outcomes, metastatic lymph node radioiodine uptake resolved completely in 191 patients (86.8%), while persistent radioiodine uptake was detected in the remaining 29 patients (13.2%) (Fig. 1B). All patients in the persistent radioiodine uptake group were classified as SIR. In the iodine uptake disappearance group, ER was the most common response category (98/191, 51.3%), followed by IDR (66/191, 34.6%), BIR (25/191, 13.1%), and SIR (2/191, 1.0%).

Figure 1

3.3 Imaging Characteristics of reLNs on Rx-WBS

On initial Rx-WBS, the median number of reLNs per patient was 3 (IQR, 1–4), and the median maximum short-axis diameter was 5 mm (IQR, 4–7). Calcification was observed in 38 patients (17.3%). The median ^{131}I uptake ratios of reLNs relative to the mediastinal blood pool and contralateral soft tissue were 88.7 and 17.7, respectively. Single-region involvement was the most prevalent pattern (147/220, 66.8%), followed by multi-region involvement (46/220, 20.9%) and isolated mediastinal involvement (27/220, 12.3%). Detailed imaging characteristics are shown in Table 2.

Table 2
Imaging characteristics of iodine-avid residual metastatic lymph nodes on Rx-WBS

Characteristics of iodine-avid reLNs	Median (IQR) / No. (%)
Number	3 (1–4)
Maximum short-axis diameter (mm)	5 (4–7)
Calcification	
Present	38 (17.3%)
Absent	182 (82.7%)
Relative iodine avidity	
Mediastinal blood pool ratio	88.7 (19.4-399.8)
Contralateral normal soft-tissue ratio	17.7 (6.1–56.4)
Regional involvement	
Single-region	147 (66.8%)
Multi-region	46 (20.9%)
Mediastinal	27 (12.3%)

Note: Data are presented as median (IQR) or No. (%). reLNs, residual metastatic lymph nodes; IQR, interquartile range; Rx-WBS, post-therapy I-131 whole-body scan with SPECT/CT.

Table 2

3.4 Factors Analysis Associated With Functional ^{131}I Therapy Response

Compared with the iodine uptake disappearance group, the persistent uptake group had a higher administered ^{131}I activity (150 vs. 120 mCi, P = 0.014), higher pre-therapy ps-Tg level (81.2 vs. 4.9 ng/mL, P < 0.001), larger maximum short-axis diameter (7 vs. 5 mm, P = 0.001), and a higher proportion of calcification (31.0% vs. 15.2%, P = 0.035). The number of iodine-avid lymph nodes was also higher in the persistent uptake group, although the difference was borderline significant (4 vs. 2, P = 0.063). The optimal cut-off values for ps-Tg was 33.75 ng/mL, maximum short-axis diameter of reLNs was 6.8 mm, and number of reLNs were 5, respectively. Other clinical and imaging variables did not differ significantly between the two groups (Table 3).

Table 3
Comparison of clinical, pathological, and imaging characteristics between the iodine uptake disappearance and persistent iodine uptake groups

Variable	Iodine uptake disappearance group (n = 191)	Persistent iodine uptake group (n = 29)	Statistic	P value
Age (years)	40 (34–51)	40 (31–52)	−0.478	0.633
Sex			**0.276**	**0.599**
Female	128 (67.0%)	18 (62.1%)		
Male	63 (33.0%)	11 (37.9%)		
Maximum primary tumor diameter (mm)	15 (9–22)	18 (12–20)	1.022	0.307
Tumor laterality			**0.363**	**0.547**
Unilateral	117 (61.3%)	16 (55.2%)		
Bilateral	74 (38.7%)	13 (44.8%)		
Cervical lymph node dissection			**2.614**	**0.106**
Central	83 (43.5%)	8 (27.6%)		
Central + lateral	108 (56.5%)	21 (72.4%)		
T stage			**0.728**	**0.917**
T1	108 (57.4%)	17 (58.6%)		
T2	27 (14.4%)	5 (17.2%)		
T3	39 (20.7%)	6 (20.7%)		
T4	14 (7.5%)	1 (3.5%)		
ATA risk stratification			**0.161**	**0.688**
Intermediate risk	159 (83.2%)	25 (86.2%)		
High risk	32 (16.8%)	4 (13.8%)		
Administered I-131 activity (mCi)	120 (100–150)	150 (120–180)	2.465	0.014*
Pre-therapy ps-Tg (ng/mL)	4.9 (0.5–15.4)	81.2 (14.6–316.0)	4.757	< 0.001*

Note: Data are presented as median (IQR) or No. (%). Comparisons involving T stage were performed after excluding Tx cases, and percentages were calculated using evaluable cases as the denominator. ATA, American Thyroid Association; ps-Tg, pre-therapy stimulated thyroglobulin; reLNs, residual metastatic lymph nodes; IQR, interquartile range. *P < 0.05.

Variable	Iodine uptake disappearance group (n = 191)	Persistent iodine uptake group (n = 29)	Statistic	P value
Imaging characteristics of iodine-avid reLNs				
Number of reLNs	2 (1–4)	4 (1–8)	1.859	0.063
Maximum short-axis diameter (mm)	5 (4–6)	7 (5–9)	3.201	0.001*
Calcification			**4.427**	**0.035***
Present	29 (15.2%)	9 (31.0%)		
Absent	162 (84.8%)	20 (69.0%)		
Mediastinal blood pool ratio	86.2 (18.0–390.1)	119.0 (24.5–709.1)	0.521	0.602
Contralateral normal soft-tissue ratio	17.4 (6.0–55.6)	24.8 (6.4–75.5)	0.469	0.639
Regional involvement			**1.111**	**0.574**
Single-region	130 (68.1%)	17 (58.6%)		
Multi-region	38 (19.9%)	8 (27.6%)		
Mediastinal	23 (12.0%)	4 (13.8%)		

Note: Data are presented as median (IQR) or No. (%). Comparisons involving T stage were performed after excluding Tx cases, and percentages were calculated using evaluable cases as the denominator. ATA, American Thyroid Association; ps-Tg, pre-therapy stimulated thyroglobulin; reLNs, residual metastatic lymph nodes; IQR, interquartile range. *P < 0.05.

Table 3

In multivariable logistic regression, pre-therapy ps-Tg (P = 0.020) and the number of iodine-avid lymph nodes (P = 0.039) were independent predictors of persistent iodine uptake after ^{131}I therapy (Table 4).

Table 4
Multivariable logistic regression models for persistent iodine uptake after I-131 therapy

Variable	OR	95%CI	*P*
I-131 activity	1.004	0.992 ~ 1.017	0.506
Pre-therapy ps-Tg	1.002	1.000 ~ 1.005	0.020*
Number	1.142	1.007 ~ 1.296	0.039*
Maximum short-axis diameter	1.057	0.927 ~ 1.205	0.405
Calcification	2.242	0.834 ~ 6.030	0.110
*Note: $P < 0.05$.			

Table 4

In the imaging-only models using either the ^{131}I uptake ratio of mediastinal or that of contralateral as the semiquantitative uptake index, lymph node number and maximum short-axis diameter of reLNs remained independently associated with persistent iodine uptake, whereas the uptake ratios were not significant predictors (Table 5).

Table 5
Multivariable logistic regression analysis of imaging features associated with persistent iodine uptake after I-131 therapy

Variable	Mediastinal ratio model			Contralateral ratio model		
	OR	95%CI	*P*	OR	95%CI	*P*
Number	1.178	1.031 ~ 1.346	0.016*	1.180	1.033 ~ 1.348	0.015*
Maximum short-axis diameter	1.126	1.008 ~ 1.258	0.036*	1.121	1.003 ~ 1.252	0.043*
Calcification	1.874	0.723 ~ 4.857	0.196	1.830	0.702 ~ 4.769	0.217
Mediastinal ratio	0.935	0.584 ~ 1.496	0.780			
Contralateral ratio				1.025	0.558 ~ 1.883	0.938
Regional involvement	0.704	0.338 ~ 1.466	0.348	0.691	0.335 ~ 1.426	0.318
*Note: $P < 0.05$.						

Table 5

3.5 Prediction Model and Nomogram for Functional ^{131}I Therapy Response

A nomogram incorporating pre-therapy ps-Tg, number of iodine-avid lymph nodes, and maximum short-axis diameter was constructed to predict persistent iodine uptake after ^{131}I therapy (Fig. 2).

Figure 2

The model showed good discrimination, with an AUC of 0.792 (95% CI, 0.678–0.906; Fig. 3A). Bootstrap calibration demonstrated good agreement between predicted and observed probabilities, with an absolute error of 0.041 (Fig. 3B). Decision curve analysis showed that the nomogram provided greater net benefit than the “treat all” or “treat none” strategies across a threshold probability range of approximately 0.10–0.90 (Fig. 3C).

Figure 3

Discussion

In this study, we evaluated therapy response after initial ^{131}I therapy in postoperative DTC patients with iodine-avid residual metastatic lymph nodes (reLNs) on Rx-WBS. Two complementary response systems were used. The ATA response-to-therapy system provides an overall clinical assessment by integrating biochemical markers and imaging findings, whereas the functional ^{131}I therapy response assessment in this study focused specifically on whether iodine-avid metastatic lymph nodes remained iodine-avid during follow-up. This distinction is important because serum Tg/TgAb and iodine imaging reflect different aspects of tumor behavior. In the present cohort, 74.5% of patients achieved an acceptable response according to ATA categories, and 86.8% showed disappearance of iodine uptake in metastatic lymph nodes, suggesting generally favorable efficacy after initial ^{131}I therapy. The discrepancies between ATA response categories and functional response were observed in some patients because ATA response-to-therapy classification integrates biochemical and imaging findings, however, functional response provides lesion-specific information on changes in iodine uptake in metastatic lymph nodes (2, 7).

The discordance between Tg and iodine imaging has been reported previously. Although pre-therapy stimulated Tg has a high negative predictive value, our previous study showed that more than half of postoperative DTC patients had discordant Tg and Rx-WBS results, and some patients still had imaging-positive residual or metastatic lesions despite sTg < 1 ng/mL (16). Other studies also reported that approximately 8%-20% of patients may show negative stimulated Tg but positive Dx-WBS or Rx-WBS findings (17). Conversely, Tg-positive but iodine scan-negative disease is also observed during follow-up and may represent an early phenotype of radioiodine-refractory disease with poorer prognosis (18). Several mechanisms may explain this discordance. Serum Tg levels are affected by tumor burden, Tg secretory capacity, TgAb interference, and assay sensitivity; in some Tg-negative patients with

metastatic disease, Tg can still be detected in fine-needle aspiration washout fluid, suggesting that serum Tg may not fully reflect small-volume nodal disease (19). In contrast, ^{131}I imaging mainly reflects iodine uptake capacity, which is closely related to sodium-iodide symporter expression and may not be synchronized with Tg synthesis or secretion (20). Therefore, relying solely on either biochemical markers or iodine imaging may underestimate the complexity of postoperative residual disease.

Our results showed that patients with persistent iodine uptake had higher pre-therapy ps-Tg levels, higher initial ^{131}I activity, more iodine-avid lymph nodes, larger maximum short-axis diameter and a higher proportion of calcified lymph nodes. In multivariable analysis, ps-Tg and the number of iodine-avid lymph nodes were independent predictors of persistent iodine uptake after ^{131}I therapy. In the imaging-only models, the number of iodine-avid lymph nodes and maximum short-axis diameter were independently associated with persistent ^{131}I uptake. These findings suggest that persistent iodine uptake is closely related to tumor burden. As a key variable in dynamic risk stratification, ps-Tg has been widely recognized as a marker of persistent or recurrent disease, with higher values indicating greater systemic tumor burden (21). Similarly, nodal number and size jointly reflect metastatic lymph node burden. Previous studies have shown that more than five metastatic lymph nodes, higher lymph node ratio, and larger metastatic lymph node diameter are associated with increased recurrence risk in DTC (22). Our findings further suggest that these nodal burden indicators are also associated with functional response after ^{131}I treatment.

Calcification was more frequent in the persistent uptake group in univariable analysis but did not remain an independent predictor after adjustment. Previous studies have reported that intranodal microcalcification and thyroid microcalcification are associated with cervical lymph node metastasis and recurrence risk (23). In the present study, the predictive value of calcification may have been weakened after adjustment for ps-Tg, lymph node number, and nodal size. Calcification may reflect long-standing or recurrent lesions and local microenvironmental changes, whereas post-treatment clearance may depend more directly on current tumor burden and radioiodine sensitivity (24).

Notably, the persistent ^{131}I uptake group received a higher initial ^{131}I activity in univariable analysis, but administered activity was not an independent predictor in multivariable analysis. This likely reflects real-world clinical decision-making rather than a causal relationship between higher activity and persistent uptake. In clinical practice, patients with higher recurrence risk, heavier tumor burden, or markedly elevated ps-Tg are more likely to receive higher ^{131}I activity (25). Therefore, the higher activity observed in the persistent uptake group probably indicates more severe baseline disease. This also highlights the need for caution when interpreting the relationship between ^{131}I activity and outcome, because persistent iodine uptake should not be simply attributed to insufficient treatment activity.

The semiquantitative ^{131}I uptake ratios, including the mediastinal blood pool ratio and contralateral soft-tissue ratio, were not independent predictors of persistent iodine uptake. One possible explanation is that higher iodine uptake has dual implications. On the one hand, it may indicate preserved iodine avidity

and potential sensitivity to ^{131}I therapy; on the other hand, it may also reflect higher tumor burden. These opposite implications may weaken its independent predictive value. Moreover, most reLNs in this study were small, with a median maximum short-axis diameter of only 5 mm. For such small lesions, SPECT/CT semiquantification may be affected by spatial resolution, partial-volume effects, ROI delineation, background selection, and image noise. Therefore, compared with more direct burden indicators such as nodal number and size, single-time-point relative uptake ratios may have limited stability for predicting functional response.

Several studies have attempted to develop nomograms for recurrence risk or ^{131}I therapy response in DTC. Li et al. incorporated pathological lymph node features such as maximum metastatic lymph node diameter, number of metastatic lymph nodes, and extranodal extension to predict structural recurrence in PTC patients with lateral neck metastasis, and their model outperformed ATA risk stratification alone (26). Wen et al. developed a nomogram using preablation stimulated Tg and the stimulated Tg/TSH ratio to predict non-ER outcomes after ^{131}I treatment in intermediate- and high-risk DTC patients (27). Other models have also used clinical factors such as age, tumor subtype, TNM stage, and Tg to predict non-ER outcomes(28). However, most existing models are based primarily on clinicopathological variables and use long-term recurrence or ATA response categories as endpoints. Few studies have integrated functional-morphological features of iodine-avid lymph nodes on postoperative Rx-WBS, and few have focused specifically on persistent iodine uptake as a functional endpoint.

In this study, we developed a nomogram based on ps-Tg, number of iodine-avid lymph nodes, and maximum short-axis diameter to predict persistent iodine uptake after ^{131}I therapy. The model showed good discrimination, with an AUC of approximately 0.79, and bootstrap calibration demonstrated good agreement between predicted and observed outcomes. Decision curve analysis further suggested that the model may provide greater net benefit than treating all patients uniformly or providing no targeted intervention across common threshold probability ranges. These results indicate that integrating biochemical and imaging features may help clinicians identify patients at higher risk of poor functional response and support individualized follow-up or retreatment decisions.

The present study is retrospective and has several inherent limitations that should be acknowledged. First, the relatively small cohort of patients with persistent iodine uptake may reduce the statistical power to identify clinically meaningful associations in multivariable analyses. Second, this study only enrolled iodine-avid metastatic lymph nodes; thus, it cannot represent the entire spectrum of persistent nodal metastatic disease. In addition, the reproducibility of semiquantitative uptake metrics may be suboptimal, especially for small lesions. Finally, given the single-center design, the generalizability of the constructed nomogram is restricted, and external validation was lacking. Accordingly, future research should focus on conducting multicenter, prospective randomized controlled trials with larger sample sizes to perform external validation prior to widespread clinical implementation.

Conclusion

For postoperative DTC patients presenting with iodine-avid residual metastatic lymph nodes, initial ^{131}I therapy achieves satisfactory therapeutic efficacy. Higher pre-therapy ps-Tg levels and a greater number of iodine-avid lymph nodes were independent predictors of persistent iodine uptake after treatment. A novel nomogram incorporating ps-Tg, metastatic nodal number, and maximum short-axis diameter was constructed to preliminarily achieve individualized prediction of functional therapeutic response, thereby guiding risk-stratified surveillance strategies for this patient cohort.

Abbreviations

AJCC
American Joint Committee on Cancer
ATA
American Thyroid Association
AUC
area under the curve
BIR
biochemical incomplete response
CI
confidence interval
CT
computed tomography
DCA
decision curve analysis
DTC
differentiated thyroid cancer
Dx-WBS
diagnostic ^{131}I whole-body scan with SPECT/CT
ER
excellent response
FTC
follicular thyroid carcinoma
IDR
indeterminate response
IQR
interquartile range
LOD
limit of detection
MRI
magnetic resonance imaging
NIS

sodium-iodide symporter
OR
odds ratio
PET/CT
positron emission tomography/computed tomography
ps-Tg
pre-therapy stimulated thyroglobulin
PTC
papillary thyroid carcinoma
RAI
radioactive iodine
reLNs
residual metastatic lymph nodes
ROC
receiver operating characteristic
SPECT/CT
single-photon emission computed tomography/computed tomography
Rx-WBS
post-therapy ^{131}I whole-body scan with SPECT/CT
SIR
structural incomplete response
Tg
thyroglobulin
TgAb
thyroglobulin antibody
TSH
thyroid-stimulating hormone
ULOQ
upper limit of quantification
VOI
volume of interest.

Declarations

Disclosure

Summary: The authors have nothing to disclose.

Declaration of competing interest

The authors declare that they have no known competing financial interests or personal relationships that could have appeared to influence the work reported in this paper.

Acknowledgments

This work was supported by generous grant from grateful patients. The authors would like to thank all the participants for their contributions in the study.

Availability of data

statement

The datasets used and/or analyzed during the current study are available from the corresponding author on reasonable request.

References

1. Fugazzola L, Elisei R, Fuhrer D, Jarzab B, Leboulleux S, Newbold K, et al. 2019 European Thyroid Association Guidelines for the Treatment and Follow-Up of Advanced Radioiodine-Refractory Thyroid Cancer. Eur Thyroid J. 2019;8(5):227–45.
2. Ringel MD, Sosa JA, Baloch Z, Bischoff L, Bloom G, Brent GA, et al. 2025 American Thyroid Association Management Guidelines for Adult Patients with Differentiated Thyroid Cancer. Thyroid®. 2025;35(8):841–985.
3. Tuttle RM, Tala H, Shah J, Leboeuf R, Ghossein R, Gonen M, et al. Estimating Risk of Recurrence in Differentiated Thyroid Cancer After Total Thyroidectomy and Radioactive Iodine Remnant Ablation: Using Response to Therapy Variables to Modify the Initial Risk Estimates Predicted by the New American Thyroid Association Staging System. Thyroid. 2010;20(12):1341–9.
4. Chidambaranathan N, Thiagarajan S, Gurukeerthi B, Sathe P, Samel P, Ramalingam N, et al. The significance of the presence of extranodal extension in the metastatic node of differentiated thyroid cancer: a proposal for modification in the American Thyroid Association (ATA) risk stratification. Eur Arch Otorhinolaryngol. 2024;281(4):1923–31.
5. Kang IK, Park J, Bae JS, Kim JS, Kim K. Lymph Node Ratio Predicts Recurrence in Patients with Papillary Thyroid Carcinoma with Low Lymph Node Yield. Cancers. 2023;15(11):2947.
6. Kang IK, Kim K, Park J, Bae JS, Kim JS. Central Lymph Node Ratio Predicts Recurrence in Patients with N1b Papillary Thyroid Carcinoma. Cancers. 2022;14(15):3677.
7. Haugen BR, Alexander EK, Bible KC, Doherty GM, Mandel SJ, Nikiforov YE, et al. 2015 American Thyroid Association Management Guidelines for Adult Patients with Thyroid Nodules and Differentiated Thyroid Cancer: The American Thyroid Association Guidelines Task Force on Thyroid Nodules and Differentiated Thyroid Cancer. Thyroid. 2016;26(1):1–133.

8. American Joint Committee on Cancer. AJCC cancer staging manual. Eighth edition, corrected at 3rd printing. Amin MB, Greene FL, Edge SB, editors. Chicago, IL: AJCC, American Joint Committee on Cancer. 2017;1032 p.
9. Guidelines Working Committee of Chinese Society of Clinical Oncology. Guidelines of Chinese Society of Clinical Oncology (CSCO) Differentiated Thyroid Cancer. J Cancer Control Treat. 2021;34(12):1164–201.
10. Gulec SA, Ahuja S, Avram AM, Bernet VJ, Bourguet P, Draganescu C, et al. A Joint Statement from the American Thyroid Association, the European Association of Nuclear Medicine, the European Thyroid Association, the Society of Nuclear Medicine and Molecular Imaging on Current Diagnostic and Theranostic Approaches in the Management of Thyroid Cancer. Thyroid. 2021;31(7):1009–19.
11. Weng HY, Yan T, Qiu WW, Fan YB, Yang ZL. The Prognosis of Skip Metastasis in Papillary Thyroid Microcarcinoma Is Better Than That of Continuous Metastasis. J Clin Endocrinol Metabolism. 2022;107(6):1589–11598.
12. Machens A, Dralle H. Correlation between the Number of Lymph Node Metastases and Lung Metastasis in Papillary Thyroid Cancer. J Clin Endocrinol Metabolism. 2012;97(12):4375–782.
13. Zhao M, Ning H, Feng M, Li S, Chang J, Qi C. Novel [99mTcN]2 + Labeled EGFR Inhibitors as Potential Radiotracers for Single Photon Emission Computed Tomography (SPECT) Tumor Imaging. Molecules. 2014;19(5):5508–21.
14. Manohar PM, Beesley LJ, Bellile EL, Worden FP, Avram AM. Prognostic Value of FDG-PET/CT Metabolic Parameters in Metastatic Radioiodine-Refractory Differentiated Thyroid Cancer. Clin Nucl Med. 2018;43(9):641–7.
15. Iasonos A, Schrag D, Raj GV, Panageas KS. How To Build and Interpret a Nomogram for Cancer Prognosis. JCO. 2008;26(8):1364–70.
16. Luo Y, Xu R, Xiao C, Xu Z, Tang C. Is ^{131}I treatment necessary for postoperative DTC patients classified as intermediate- or high-risk with negative stimulated thyroglobulin? Appl Radiat Isot. 2025;226:112190.
17. Cherk MH, Francis P, Topliss DJ, Bailey M, Kalff V. Incidence and implications of negative serum thyroglobulin but positive I-131 whole-body scans in patients with well-differentiated thyroid cancer prepared with rhTSH or thyroid hormone withdrawal. Clin Endocrinol. 2012;76(5):734–40.
18. Kloos RT. Approach to the Patient with a Positive Serum Thyroglobulin and a Negative Radioiodine Scan after Initial Therapy for Differentiated Thyroid Cancer. J Clin Endocrinol Metabolism. 2008;93(5):1519–25.
19. Andress B, Miller SA, Maus AD, Kemp JV, Bornhorst JA, Grebe SK, et al. Undetectable Serum Thyroglobulin in Patients With Differentiated Thyroid Cancer: Antithyroglobulin Antibodies, Assay Limitation, or Other? Endocr Pract. 2025;31(10):1286–91.
20. Müller-Gärtner HW, Schneider C. Clinical evaluation of tumor characteristics predisposing serum thyroglobulin to be undetectable in patients with differentiated thyroid cancer. Cancer. 1988;61(5):976–81.

21. Xue Y, Zheng M, Wu X, Li B, Ding X, Liu S, et al. A digital pathology model for predicting radioiodine-avid metastases on initial post-therapeutic ^{131}I scan in patients with papillary thyroid cancer. Sci Rep. 2024;14(1):26786.
22. Palacardo F, Lee-Saxton YJ, Tumati A, Marshall TE, Greenspun BC, Zarnegar R, et al. The Impact of Radioactive Iodine on Disease-Specific Survival in Low-to-Intermediate Risk N1b Papillary Thyroid Carcinoma. Ann Surg Oncol. 2025;32(3):1698–708.
23. Liu XN, Duan YS, Wu YS, Brogna MR, Domínguez-Ayala M, Di X, et al. Correlation between ultrasound calcification patterns, and clinicopathological factors and recurrence risk in papillary thyroid carcinoma. Gland Surg. 2025;14(9):1821–34.
24. Xing Z, Qiu Y, Li Z, Zhang L, Fei Y, Zhu J, et al. Predictors of thyroglobulin in the lymph nodes recurrence of papillary thyroid carcinoma undergoing total thyroidectomy. BMC Surg. 2021;21(1):53.
25. Nguyen NC, Anigati EM, Desai NB, Öz OK. Radioactive Iodine Therapy in Differentiated Thyroid Cancer: An Update on Dose Recommendations and Risk of Secondary Primary Malignancies. Semin Nucl Med. 2024;54(4):488–96.
26. Jianyong L, Jinjing Z, Zhihui L, Tao W, Rixiang G, Jingqiang Z. A Nomogram Based on the Characteristics of Metastatic Lymph Nodes to Predict Papillary Thyroid Carcinoma Recurrence. Thyroid. 2018;28(3):301–10.
27. Wen R, Zhao M, Chen C, Yang Y, Zhang B. A novel nomogram integrated with preablation stimulated thyroglobulin and thyroglobulin/thyroid-stimulating hormone ratio to predict the therapeutic response of intermediate– and high–risk differentiated thyroid cancer patients: a bi-center retrospective study. Endocrine. 2023;84(3):989–98.
28. Cao J, Liang H, Li X, Guan X, Xu H. A clinical feature–based nomogram for the personalized prediction of radioactive iodine therapy outcomes in patients with papillary thyroid carcinoma. Oncol Lett. 2025;30(6):1–12.

Figures

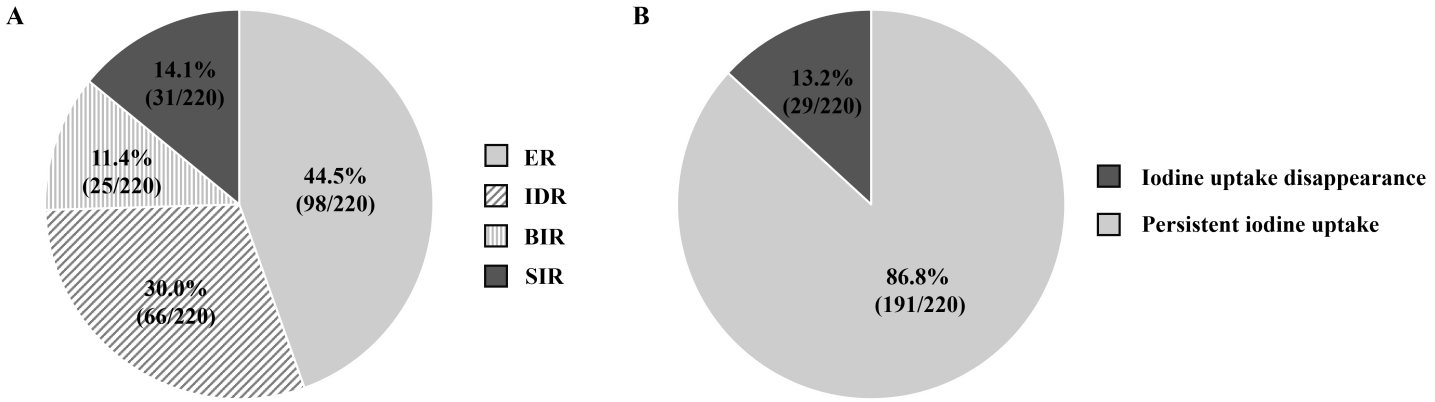


Figure 1

Distribution of response-to-therapy categories and functional response after initial ^{131}I therapy. (A) Distribution of ATA response-to-therapy categories, including ER, IDR, BIR, and SIR. (B) Distribution of functional therapy response according to the iodine uptake status of metastatic lymph nodes during follow-up.

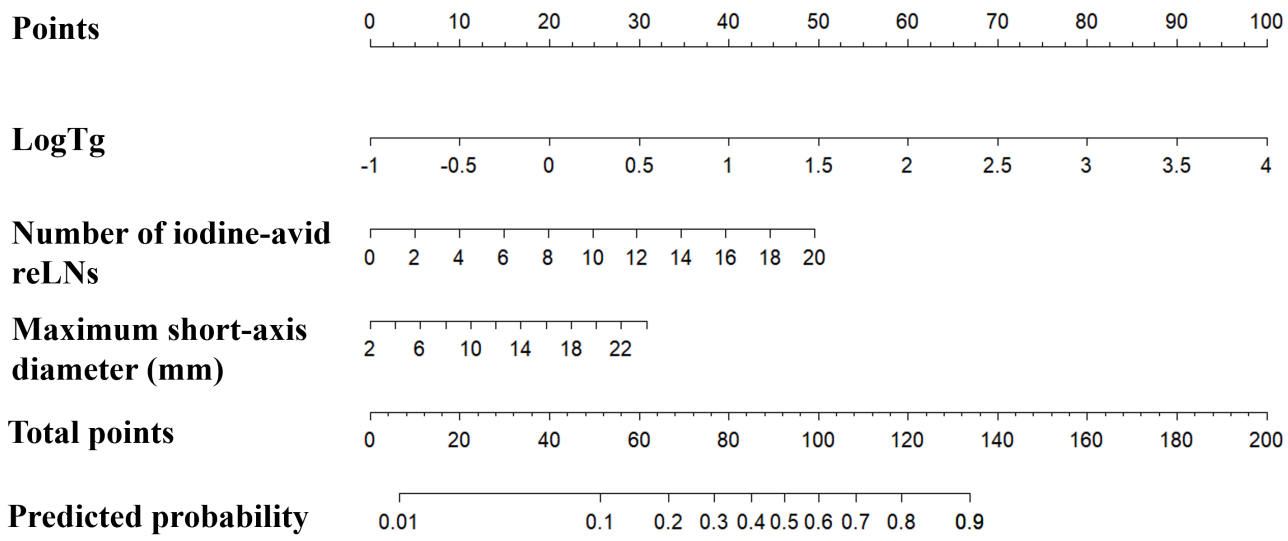


Figure 2

Nomogram for predicting persistent iodine uptake in metastatic lymph nodes after initial ^{131}I therapy. The nomogram was constructed using pre-therapy stimulated thyroglobulin (ps-Tg), the number of iodine-avid lymph nodes, and maximum short-axis diameter. The total points correspond to the predicted probability of persistent iodine uptake in metastatic lymph nodes after treatment. LogTg indicates log10-transformed pre-therapy ps-Tg.

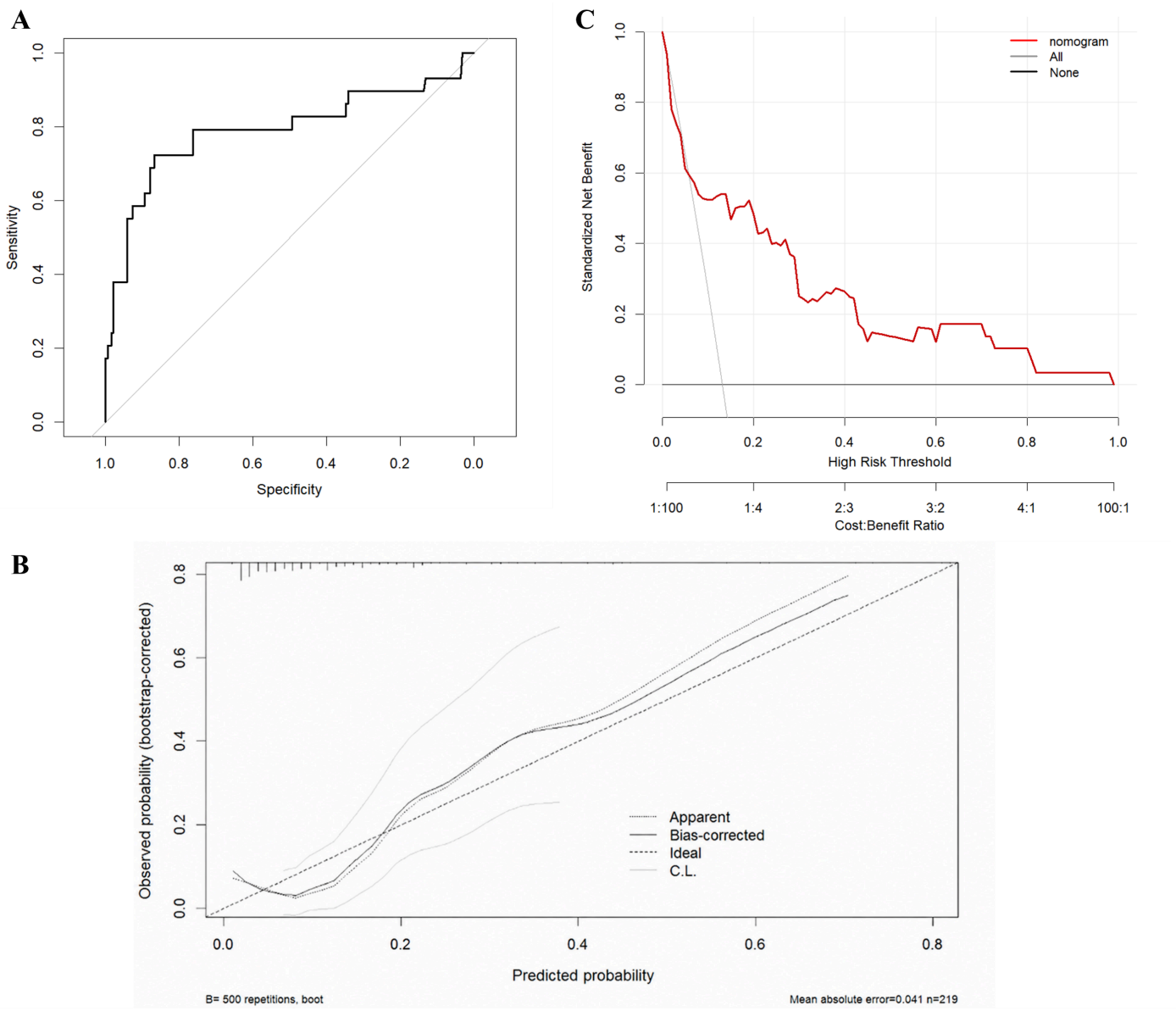


Figure 3

Performance evaluation of the nomogram for predicting persistent iodine uptake after initial ^{131}I therapy. (A) Receiver operating characteristic curve of the prediction model. The area under the curve was 0.792 (95% CI, 0.678-0.906). (B) Calibration curve based on bootstrap validation, showing the agreement between predicted and observed probabilities. (C) Decision curve analysis showing the net benefit of the nomogram across different threshold probabilities compared with the “treat all” and “treat none” strategies. ROC, receiver operating characteristic; AUC, area under the curve; DCA, decision curve analysis.